Applied Water Science (2022) 12:86
https://doi.org/10.1007/s13201-022-01588-5

ORIGINAL ARTICLE

Removal of of toxic metal ions (Ni^{2+} and Cd^{2+}) from wastewater by using TOPO decorated iron oxide nanoparticles

Sosun[1] · Attarad Ali[2] · Abdul Mannan[3] · Usman Ali Shah[3] · Muhammad Zia[1]

Received: 5 November 2021 / Accepted: 7 February 2022 / Published online: 4 April 2022

Abstract

In real engineering applications, nanoparticles can face hurdles of complex behavior of pollutants, for which electrostatic forces and background electrolyte can prove to be one of the robust mechanisms to remove pollutants from wastewater. In the present work, magnetite (Fe_3O_4) nanoparticles (NPs) and trioctyl phosphine oxide (TOPO) coated Fe_3O_4 NPs were synthesized and characterized for removing divalent Ni^{2+} and Cd^{2+} ions. Morphological and chemical analysis of both NPs was performed, and batch adsorption experiments were performed to study the influence of different pH ranges, concentrations of adsorbents and different contact timings. TOPO functionalized magnetite nanoparticles were found to have better adsorption capacities as compared to Fe_3O_4 at higher pH values. Isotherm models were run to identify the adsorption process. Langmuir isotherm model data fitted best for both metal ions adsorption, while Freundlich data suited best only for Ni^{2+} ions. The regression values for kinetic models confirmed that pseudo-second-order fitted best to the adsorption of both Ni^{2+} and Cd^{2+}. Higher adsorption values were noticed for Ni^{2+} at higher dosages of both bare and TOPO-coated iron oxide NPs. Cadmium was found to have no influence of adsorbent dosage. Contact time was found to impact sorption values, i.e., adsorption was greater initially and then decreased with the passage of time. The study concludes that TOPO decorated Fe_3O_4 NPs can be more efficiently used for wastewater treatment. Furthermore, the presence of alkyl chains in TOPO can be immobilized at surface of metals to undergo adsorption more efficiently.

Keywords Trioctyl phosphine oxide (TOPO) · Adsorption · Heavy metals · Iron oxide · Wastewater · Isotherm · Kinetics · Batch reactions

Introduction

Water is one of the most crucial renewable resources for sustenance of all sorts of life, food and economic growth (Singh and Gupta 2016).In the present time, the need for water in anthropogenic work has risen up due to growing population. This increased urbanization and rapid fleet of industrialization are ultimately resulting in pollution of water and soil as indicated in Fig. 1, respectively (Vardhan et al. 2019). Anthropogenic activities like agriculture, industry, mining and smelting can result in gradual accumulation of heavy metals in the environment (Sardar et al. 2013). Heavy metal refers to the group metals and metalloids that have density greater than 4 ± 1 g/cm^3(Mohammed et al. 2011). However, more important than their density is their chemical properties that need serious attention in order to combat the threats they imply to all life forms. Heavy metals include lead (Pb), cadmium(Cd), zinc(Zn), mercury(Hg), silver(Ag), chromium(Cr) and copper(Cu)

✉ Attarad Ali
attarad.ali@uo.edu.pk

Sosun
Sosunkhan786@gmail.com

Abdul Mannan
abdulmannan_ka@yahoo.com

Usman Ali Shah
usman_ali_shah@gmail.com

Muhammad Zia
ziachaudhary@gmail.com

[1] Department of Biotechnology, Quaid-i-Azam University, Islamabad 45320, Pakistan

[2] Directorate of QEC (Quality Enhancement Cell), University of Baltistan Skardu Gilgit-Baltistan (GB) Pakistan, Skardu 16100, Pakistan

[3] Department of Pharmacy, COMSATS University, Abbottabad, Pakistan

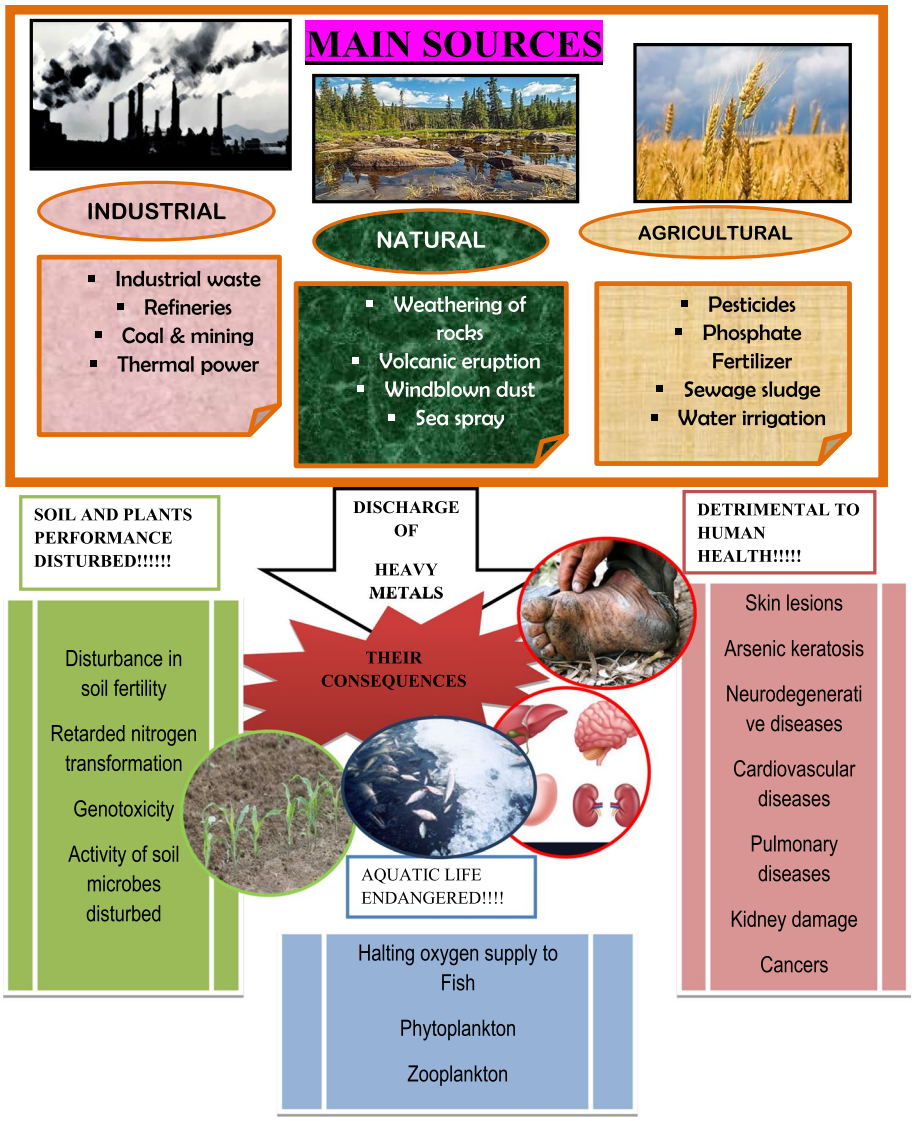

Fig. 1 Sources and consequences of heavy metals on all life forms (Srivastava et al. 2017; Jaishankar et al. 2014; Gheorghe et al. 2017)

and metalloids such as arsenic(As) (Duruibe et al. 2007). These metals can jeopardize human's, microbe's and plant's life. They are recalcitrant to many biochemical reactions and thus difficult to remove. Even low concentrations of heavy metals can interfere with plant living system and may cause cancer in humans. They can produce ROS(reactive oxygen species) that suffocates underwater life (fishes and aquatic plants) (Singh and Kalamdhad 2011; Baragaño et al. 2020). Common methods for the removal of heavy metals include adsorption, ion exchange, filtration, biosorption, coagulation and cementation (Masindi and Muedi 2018) (Fig. 2).

In such a scenario, there is a need to introduce a system that would ensure robust elimination of heavy metals. Recently, nanoremediation has proved to be very effective for better adsorption efficiencies, low cost and durability of clean-up process as there is no need to pump ground water to surface site or transporting soil from one place to other (Rajendran and Sen 2018). Iron-based nanoparticles such

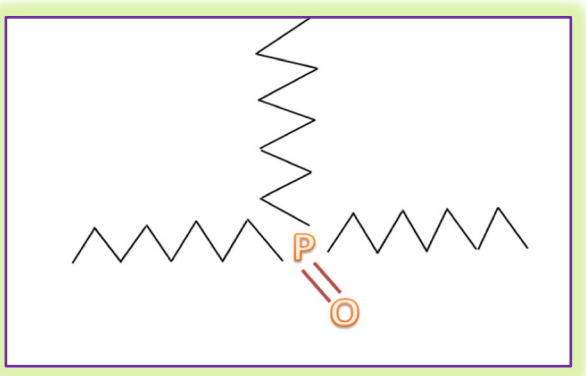

Fig. 2 Typical structure of trioctyl phosphine oxide TOPO (Three octyl chains and one phosphine oxide group) [Chemical Book, TOPO 2017]

as nano-zero valent ion (nZVI) are found to be competing with most renowned techniques of in situ bioremediation and chemical reduction (Bardos 2015). Iron oxide nanoparticles due to their infinite surface area and accurate sizes can result in greater degree of adsorption to various heavy metals says Al-Saad et al. (2012).

Iron oxide nanoparticles are selected as they offer a number of advantages including their inert and non-toxic thus making it easier to apply their magnetic properties in environmental regimes. Their abundant occurrence in earth makes it feasible and cost-effective approach to use. Targeting of site-specific contaminated zone through magnetic support is another advantage. Moreover, the process of adsorption occurs on external surface of iron oxide thus ensuring less adsorption time (more kinetic rates). Iron oxide has high surface-to-volume ratio thus providing more active sites for the heavy metal to attach. Moreover, it becomes easier to separate the adsorbate liquid by magnetic force. Iron oxide nanoparticles are reusable. They are highly dispersed in liquid system thus not involving the problems of membrane fouling, high-pressure treatment and packed column plugging (Nassar 2012).

Surface functionalization is the very first requirement for the real applicability of iron oxide nanoparticles. Thus promising extended stability and withstanding harsh conditions of pH and electrolyte. The famous Derjaguin–Landau–Verwey–Overbeek (DLVO) theory is used to find out the interaction capacity around the surface of a particle. The colloidal stability of nanoparticles is assigned to the balance between repulsive and attractive forces. For iron oxide nanoparticles, these attractive forces are due to Van der Waal forces and magnetic forces of nanoparticles acting as magnetic dipoles (Walter et al. 2015).

In order to control the aggregation and interactions of bare iron oxide nanoparticles, they are often treated with surfactants such as TOPO (Trioctyl phosphine oxide). TOPO (properties are briefly given in Table 1) is an organophosphorus compound and a white crystalline solid used as stabilizing agent for a variety of nanoparticles (Chemical Book, TOPO 2017). TOPO was considered as an attention-grabbing laboratory compound since 1970's when for the first time it was used at Oak Ridge National Laboratory scientists recovered uranium from the wet process phosphoric acid. Apart from this TOPO was used for recovery of organics from fermentation broth (Watson and Rickelton 1992).

In the present study, magnetite nanoparticles conjugated to TOPO were used as an adsorbent system to remove cadmium and nickel heavy metals from synthetic wastewater solutions. Magnetite nanoparticles due to their abundant nature and high capacity for adsorbing heavy metals can be used along with TOPO as stabilizing agent that proves to be one of the efficient removal systems so far in nanoremediation.

Methods

Materials

Ferrous sulphate hepta hydrate $FeSO_4.7H_20$ (Molecular weight: 278.02 g/mol), Sodium borohydride $NaBH_4$ (Molecular weight: 37.83 g/mol), n-Hexane, Trioctylphosphine oxide (TOPO) (Molecular weight:386.6 g/mol), Cadmium nitrate $Cd(NO_3)\cdot 4H_2O$ (Molecular weight:308.48 g/mol), Nickel (II) Chloride $NiCl_2.6H_2O$ (Molecular weight:237.73 g/mol).

Experiment

Surface functionalization of iron oxide nanoparticles with trioctylphosphine oxide (TOPO)

5 Mm TOPO (Trioctylphosphine oxide) was prepared in a 100 ml flask containing 25 ml hexane. 2.5 g of iron salt (Ferrous sulphate) was added to 200 ml distilled water and stirred for 30 min to prepare a true solution. TOPO solution was then added to the iron salt solution and stirred for 1 h at maximum speed. Following this, the above solution was then added to ice cold $NaBH_4$ (1%). Color change was observed from yellow to blackish brown. Purification of pellets was undergone through centrifugation at 10,000 rpm for 10 min and washed three times with distilled water. The pellets were then dried in a drying oven at 50 °C for 2 days. Afterward, the TOPO bound iron oxide nanoparticles were scratched and powdered through pestle and mortar to make a fine powder which was then subjected to characterization.

Preparation of artificial waste water

Artificial water samples were prepared by mixing standard heavy metal solutions of cadmium nitrate $Cd(NO_3)4H_2O$ and nickel chloride $NiCl_2\cdot 6H_2O$ salt solutions. Stock solutions of these heavy metal solutions were prepared by mixing 10 mg of both the salts to 1000 ml distilled water.

Batch adsorption experiments

Batch adsorption experiments were performed in the laboratory of Nano biotechnology lab of Quad-i-azam University, Islamabad, Pakistan. The aim of the present work was to explore as how increase or decrease in pH can affect the adsorption phenomena of the divalent ions on the surface of magnetite NPs and TOPO bound magnetite NPs. Stock solutions of salts cadmium nitrate and nickel chloride 10 mg each separately mixed in 1000 ml distilled water out of which sets of experiments were performed for elucidating the effect of different pH (5, 6, 7, 8) at different time intervals using a pH meter equipped with electrodes.1 M sodium hydroxide NaOH

and 1 M hydrochloric acid HCl were used for balancing the pH levels to desirable values by adding them dropwise with the help of separate droppers. Dose of adsorbent iron oxide nanoparticles (IONPs sample and Fe_3O_4 + TOPO sample) was 2 mg/20 ml (for pH 5, 6, 7, 8) and 4 mg/40 ml (pH6). As soon as the desirable pH values were maintained adsorbent was added to the wastewater and stirred on magnetic stirrer at maximum speed 800 rpm and 25 °C to reach equilibrium conditions. Contact time was 50 min for adsorbent dosage 2 mg/20 ml metal solution and 100 min for adsorbent dosage 4 mg/40 ml metal ion solution, respectively. Concentrations of Ni^{2+} and Cd^{2+} ions were determined by first collecting 10 ml and 20 ml of solutions after every 10 min and then analyzing them using atomic absorption spectrometer on flame mode. In the present study, Shimadzu model AA-670/g V-7 Atomic absorption spectrometer with deuterium lamp background correction and hollow cathode lamps at respective wavelengths as radiation sources was employed throughout the measurements. An air acetylene flame was used for determination of nickel and cadmium ions. Calibration curves for both the metals were constructed, and their respective absorbance values were obtained in graphical form as concentration versus absorbance.

Modeling of sorption equilibrium and kinetic data

From the calibration curves, the absorbance values gave the concentrations of nickel and cadmium ions. These concentration values were then used in equilibrium studies to check the adsorption behavior of respective metal ions. For studying pathway of adsorption and equilibrium correlation between adsorbent and adsorbate, it is important to establish equilibrium isotherms (Batool etal. 2018). Adsorption isotherm models were thus applied onto the concentrations of metals in order to find the amounts of solute (metals) adsorbed on the surface of solid (q_e) mg/g and the amount of solute in liquid (C_e)mg/l. On the other hand, kinetic models were applied to reveal the sorption rates of metal ions. Two types of kinetic equations are commonly compared, called as pseudo-first-order kinetics and pseudo-second-order kinetics. Pseudo-first-order kinetic (PFO) model was discovered by Lagergren denoted by $K1$, whereas pseudo-second-order (PSO) model was discovered in mid-1980. It is denoted by $K2$[2]. Analysis of a number of research articles done by (Ho and McKay 1999) reached a conclusion that majority of systems studies, PSO provides the perfect correlation of experimental data. After this piece of work, $K2$ has become the most superior in kinetic studies (Simonin 2016). The adsorption capacities at any time (q_t, mg/g) and at equilibrium (q_e, mg/g) are calculated using the following equations.

$$q_e = \left(C_0 - C_e\right)V/m \tag{1}$$

$$q_t = \left(C_0 - C_t\right)V/m \tag{2}$$

Langmuir isotherm Theoretical model developed by Irving Langmuir in 1916 is the most widely employed isotherm model for adsorption studies. Basic concept of this model is the monolayer coverage of the adsorbate on homogenous surface. This model assumes that all sites of adsorbent are homogenous and the forces of interaction are minor. Therefore, once the adsorption takes place and occupied by molecules in all respective (homogenous) sites of the adsorbent, then further no adsorption occurs (Chowdhury et al. 2011; Terdputtakun et al. 2017).

Linear equation for Langmui model is written as $1/q_e$

$$= 1/Q_m + 1/bQ_m + 1/C_e \tag{3}$$

With the help of Microsoft Excel 2010, linear graphs were constructed as C_e/q_e versus C_e.

Q_e value was calculated from the formula $Q_e = Q_m.b.$ Ce/1 + $b.C_e$. This Q_e is actually the least sorption capacity of adsorbent (on peak time interval) at equilibrium (after which desorption starts). The linear graph will produce $y = mx + c$. Where m is the intercept equal to $1/b$.Qm and slope = $1/Q_m$.

Freundlich isotherm In the presence of multiple layers or sites available for adsorption, the Langmuir model is unable to explain the adsorption phenomena, and therefore, Freundlich isotherm model is applied to explain heterogeneous adsorption behavior on the surface of adsorbent. In 1909, Freundlich explained the first mathematical model to a nonlinear isotherm resulting into a pure empirical formula for adsorption on heterogeneous sites (Rahbaralam et al. 2020).

Equation for Freundlich isotherm is written as $\log q_e$

$$= \log Kf + 1/n \log C_e \tag{4}$$

From the above equation, Freundlich plots were constructed as $\log q_e$ against $\log C_e$.

Q_e value was calculated via the formula $Q_e = Kf$ Ce $1/n$. Slope = 1/Qm and Intercept = $1/b\ Q_m$.

Pseudo-first-order kinetics Equation for pseudo-second-order kinetic model is given as

$$\log\left(q_e - q_t\right) = \log\left(q_e\right) - (k1/2.303)\,t. \tag{5}$$

Plot constructed as $\log(q_e - q_t)$ versus time(t). This gives a slope equal to $-k/2.303$ and an intercept equal to $\log(q_e)$.

Pseudo-second-order kinetic Equation for pseudo-second-order kinetic model is written as

$$t/q_t = 1/k2q_e^2 + \left(1/q_e\right)t \tag{6}$$

$k1$ (/min) and $k2$ (g/mg min) are the pseudo-first-order and second-order rate constant.

The linear plots of pseudo-first-order and pseudo-second-order kinetics were used to calculate the values of kinetic parameters.

q_t is amount of cadmium ion and nickel ion on the surface of iron oxide and TOPO Functionalized iron oxide NPs at any time, t,(mg/g). h is the initial sorption rate. ($h = qt/t$) when t approaches 0, then h (mg/g min) becomes kq^2_e. Values of k and h are determined from slope and intercept as $k = \text{slope}^2/\text{intercept}$ and $h = 1/\text{intercept}$.

Regression analysis

In the present study, linear regression analysis was done to determine the values of isotherm and kinetic model parameters. The values of correlation coefficient (R2) were obtained from the graphs generated by using Microsoft Excel 2010. Through this value, it was studied which isotherm or kinetic model best fits the data. Higher the values of R^2, more appropriate the data are value of regression coefficient that may vary from 0 to 1 (Sogut and Caliskan 2017). R^2 values were generated through the following Eq. (6) (Chen 2015).

$$R^2 = \frac{\left(q_m - \overline{q_e}\right)^2}{\left(q_m - q_e\right) + \left(q_m - \overline{q_e}\right)^2} \tag{7}$$

where q_e is the equilibrium capacity obtained from experiments, q_m is the constant obtained from isotherm model, and $\overline{q_e}$ is the average of q_e, respectively.

Results and discussion

Characterization of adsorbents

XRD study

Crystal structure and average diameter of nanoparticles were analyzed through X-ray diffraction. XRD patterns of each sample are shown Fig. 3. Characteristic diffraction peaks of the iron oxide nanoparticles are 30.12, 35.59, 43.15, 57.25 and 62.45 which, respectively, corresponds to (220), (311),(400), (511) and (440) planes of magnetite nanoparticles. Same results were found in work of (Mazrouaa et al. 2019). Also, these XRD peaks are in accordance with the (JCPDS 19-629). The TOPO functionalized iron oxide nanoparticles are showing their respective peaks on 30.12, 35.69, 43.84 and 62.17 (at 2θ degrees) which coincide with hkl plane of cubic magnetite as 220, 311, 400 and 400 respectively, obtained from its JCPDS Card No.19-0629 (Rusianto et al. 2015).

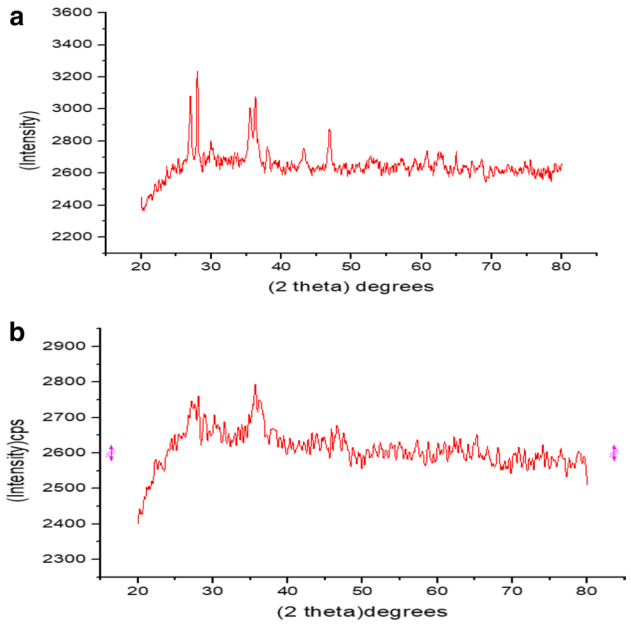

Fig. 3 X-ray diffraction pattern of (**a**) magnetite nanoparticles and (**b**) TOPO (Trioctylphosphine oxide) functionalized magnetite nanoparticles

FTIR study

The characteristic peaks of Fe–O bonding in iron oxide sample are found at ranges of 579 cm^{-1}. For nanoparticles to be magnetite in nature, they need to display FTIR peak at 580 cm^{-1} (Petcharoen and Sirivat 2012). Absorption band at 3354 cm^{-1} might be due to the moisture content absorbed by the nanoparticles from atmosphere. Bands at 1320–1000 indicate C–O stretches (Fig. 4a). The peaks corresponding to TOPO functionalized nanoparticles were found around at 996 cm^{-1} range for the presence of phosphine oxide functional group i.e., being found in TOPO molecule. Same results were reported by (Xu et al. 2011). Another study done by Zhang et al. (2012) confirms that the peaks around 990–1300 cm^{-1} confirm the attachment of functional group P = 0 in TOPO. Peaks around 579 cm^{-1} range are characteristic of Fe–O bond in magnetite nanoparticles. Bands at 3165 cm^{-1} might be due to the terminal alkyl groups; C–H stretches (Fig. 4b). A similar study says that for TOPO functionalized iron oxide additional peaks at around 2926 cm^{-1} confirm the attachment of TOPO (Batra and Datta 2019).

SEM study

Morphological studies of samples were done using high-resolution scanning electron microscopy. Sample of iron oxide presented a large number of dispersive cubic structured nanoparticles. SEM micrographs are presented in Fig. 5 where the TOPO functionalized nanoparticles

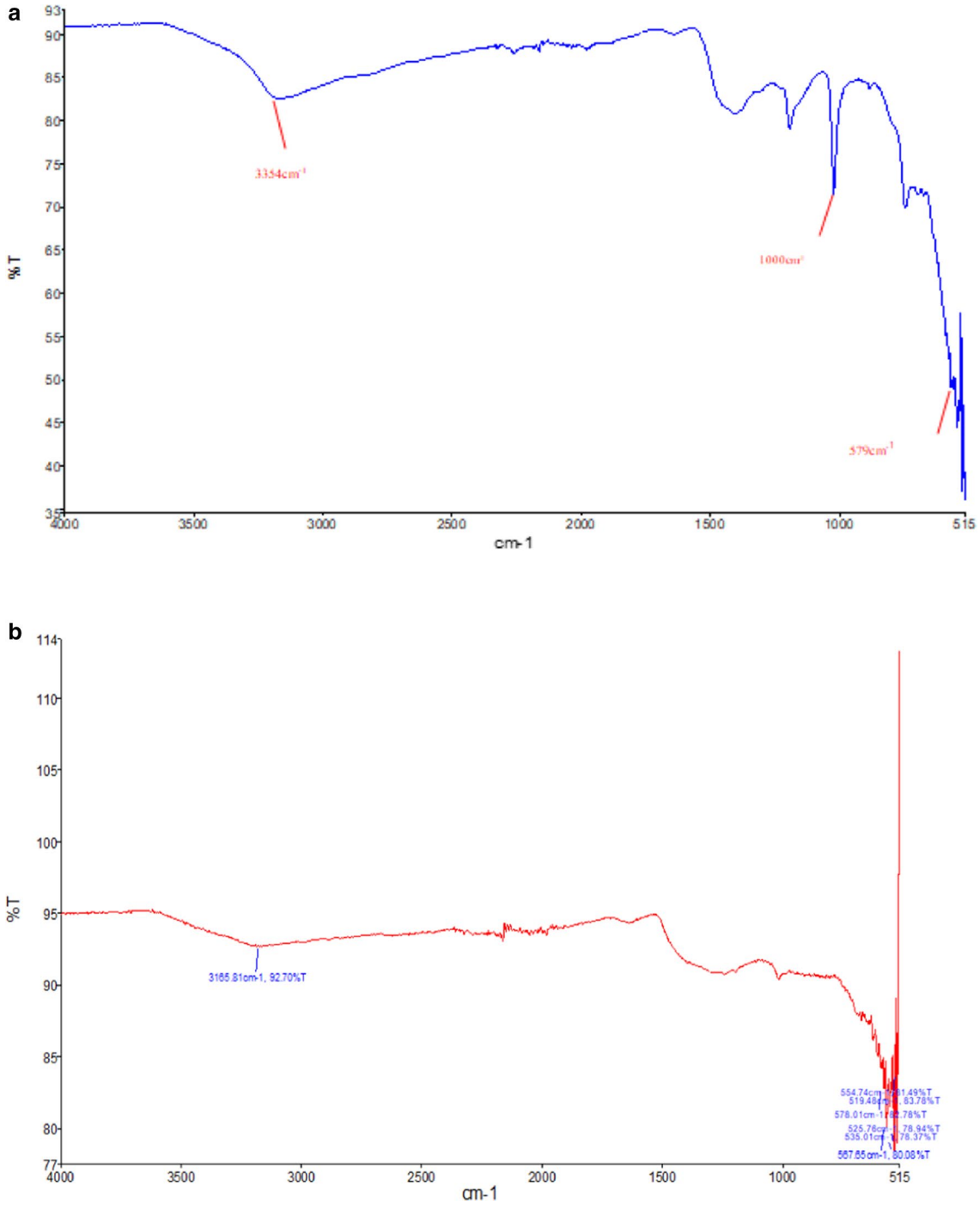

Fig. 4 FTIR spectra of (**a**) iron oxide and (**b**) TOPO functionalized iron oxide nanoparticles

displayed cubic spinel structures with efficient attachment of white crystalline trioctyl phosphine oxide. Thus, the SEM images of iron oxide NPs confirm that they are in nanoscale range and trioctyl phosphine oxide is effectively conjugated to iron oxide NPs. Same results were found in the work of Alatorre et al. (2019). They employed non-conventional chemical method using external magnetic field to synthesize iron oxide nanoparticles. Same SEM images were found in a study by Lim et al. (2014) who used ferrous sulphate and ferrous nitrate as salt precursors in the presence of NaOH to synthesize iron oxide nanoparticles. In another study, Li et al. (2017) generated cube-like nanoparticles by two-stage oxidation method and sphere like by single-stage oxidation method.

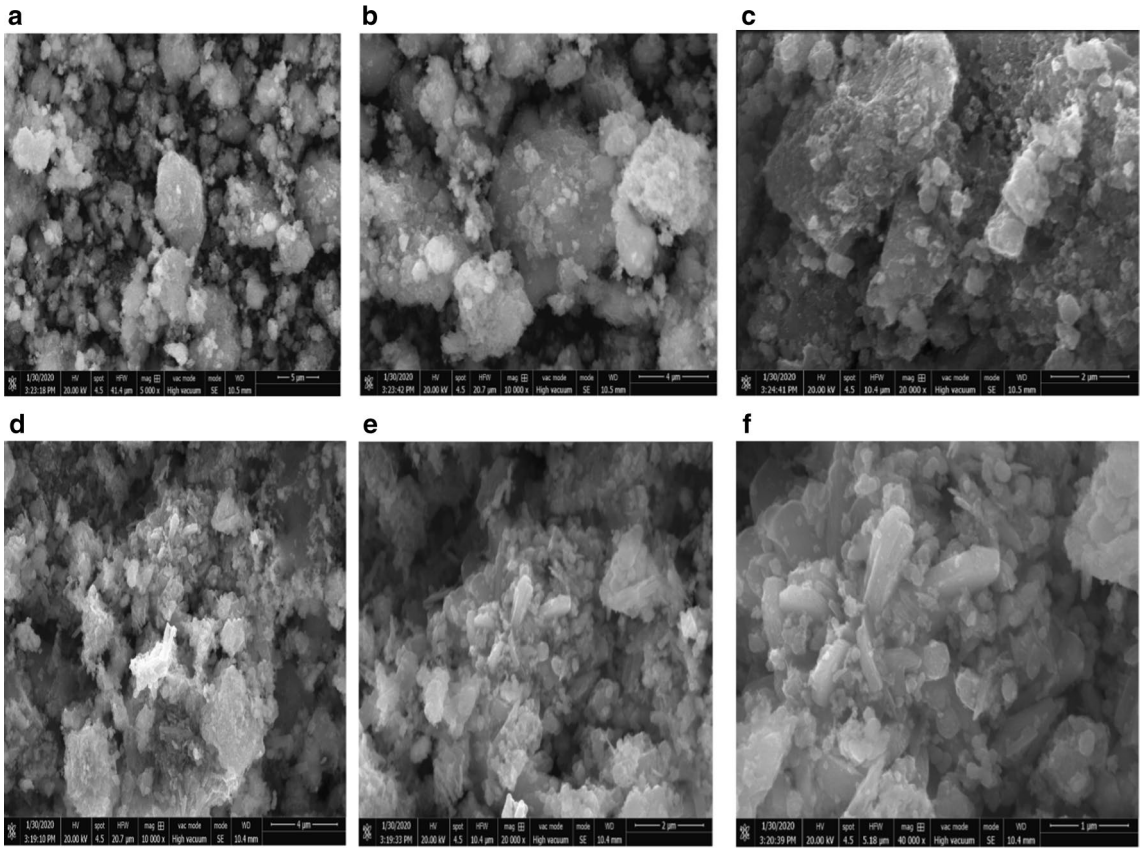

Fig. 5 SEM images of iron oxide NPs at (**a**) 5000× (**b**) 10000× (**c**) 20000× Magnification and TOPO Functionalized NPs at (**d**) 10000× (**e**) 20000× (**f**) 40000× Magnification

Adsorption isotherms

Fitting of adsorption isotherms equation to experimental data is the most crucial step in data analysis (Kinniburgh 1986). Adsorption isotherm is an empirical relationship employed to analyze the amount of solute (adsorbate) adsorbed on adsorbent. Adsorption isotherm is a graph that reveals the relationship between amount adsorbed by a unit gram of sorbent and the amount of metal ions left in an experimental medium after equilibrium along with distribution of metal ions between solid and liquid phases (Desta 2013). Among isotherm models, Langmuir and Freundlich adsorption isotherms models are the most widely studied. The Langmuir model is associated with monolayer coverage onto the adsorption sites, whereas Freundlich isotherm is associated with reversible adsorption and explains heterogeneous surface of adsorption (Khajavian et al. 2019). In the present study, Langmuir and Freundlich isotherm models were applied to find equilibrium(Q_e) between heavy metals cadmium and nickel on iron oxide nanoparticles (IONPs) and TOPO functionalized nanoparticles (TF IONPs) and the ion's concentration (C_e) at constant temperature. Linearized form of Langmuir and Freundlich isotherms is stated in Eqs. (9) and (11) (Table 1).

Table 1 Chemical properties of TOPO. Retrieved from National library of Medicine, [PubChem]. [Chemical Book, TOPO 2017]

Name of features	Description
Molecular formula	C24H51OP
IUPAC Name	1-dioctylphosphoryloctane
Exact Molecular mass	386.367753 g/mol
Topological surface area	17.1Å^2
Form	White/yellow crystalline powder
Density	0.88 g/cm^3
Melting point	50–52 °C
Boiling point	201–202 °C
Solubility	Less than 1 g/L

Langmuir isotherm

The Langmuir isotherm model assumes the formation of monolayer of metal molecules on the outer surface of adsorbent after which no further adsorption takes place on adsorbent surface. It explains the equilibrium distribution of metal ions between liquid and solid phases (Dada et al. 2012). Mathematically, the equation is given as

$$q_e = \left(bQ_mC_e\right)/\left(1 + bC_e\right) \tag{8}$$

Linearized form :

$$C_e/q_e = \left(C_e/Q_m\right) + 1/bQ_m \tag{9}$$

where q_e is solute(adsorbate) uptake per unit weight of iron oxide and functionalized iron oxide nanoparticles(mg/g) at equilibrium solute concentrations, C_e is the equilibrium concentration of adsorbate in solution (mg/L), and Q_m and b are Langmuir constants associated with the sorption capacity and energy of adsorption, respectively. The plots of C_e/q_e versus C_e show that adsorption of Ni^{2+} and Cd^{2+} gives a straight line which is represented in (Fig. 6a–d).Values of qm and b of the linear equation of Langmuir adsorption isotherm were derived from the slopes and intercepts of the

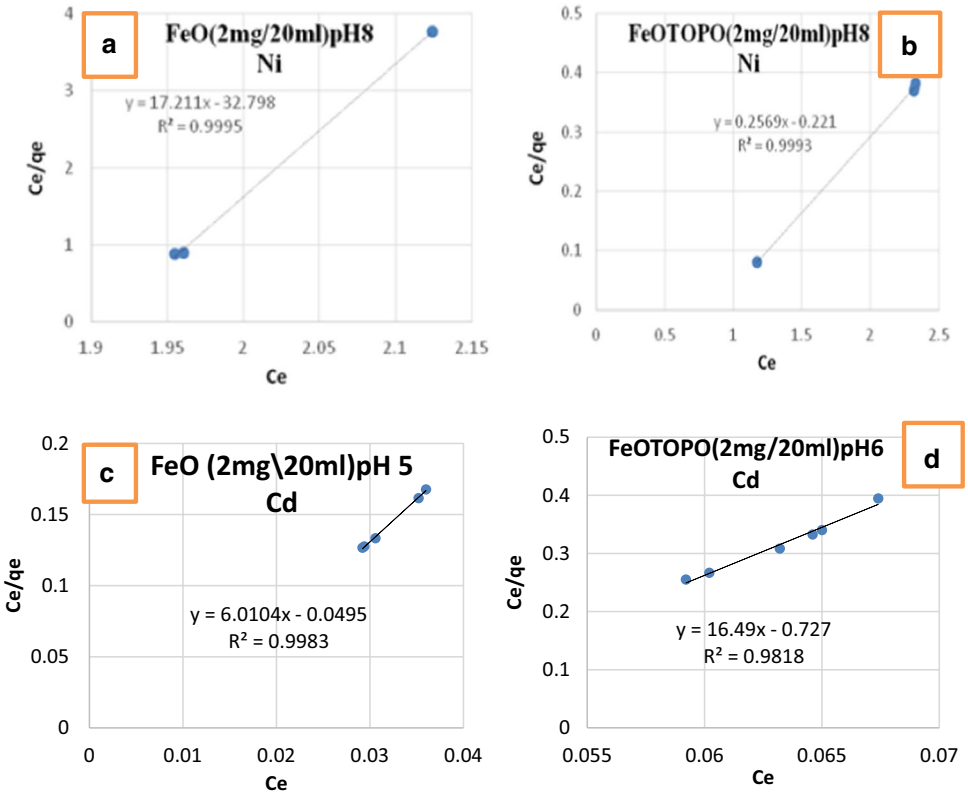

Fig. 6 Langmuir isotherm plots for adsorption of (**a**) magnetite NPs (2 mg/20 ml) to Cd at pH8, (**b**) TOPO coated magnetite NPs (2 mg/20 ml) to Ni at pH8, (**c**) magnetite NPs (2 mg/20 ml) to Cd at pH5 (**d**) TOPO coated magnetite NPs to Cd at pH 6

Table 2 Parameters of isotherm adsorption models for adsorption of nickel metal ions on iron oxide and TOPO functionalized iron oxide nanoparticles at 25 °C and different pH ranges, i.e., 5, 6, 7, and 8

pH range	Langmuir parameters			Freundlich parameters		
	R^2	Q_m	b	Q	R^2	Kf
For FeO 2 mg/20 ml nickel metal ion						
pH5	0.9527	0.006394271	0.832304417	0.747216618	0.9987	0.51315184
pH6	0.9956	0.003153977	0.400991539	0.108225108	0.9978	2.511645273
pH7	0.9664	1.669727834	0.438337115	0.356544372	0.9883	1.497783827
pH8	0.9995	0.058102376	0.524757607	0.611845326	0.9998	3.21535649
For FeO 4 mg/40 ml						
pH6	0.5655	0.315000315	0.485093899	0.233198078	0.9646	1.882870306
For FeO TOPO 2 mg/20 ml						
pH5	0.8912	0.018933298	0.948444907	0.044901441	0.9698	33.37479395
pH6	0.9963	0.880049283	0.478704133	0.187286961	0.9987	1.859705339
pH7	0.9949	0.326541275	0.815791577	0.16677507	0.9995	3.939618922
pH8	0.9993	3.8925652	1.162443439	0.444385193	1	1.704514468
For FeO TOPO 4 mg/40 ml						
pH6	0.5899	4.723665564	0.501539919	0.449357419	0.7501	1.029277092

Table 3 Parameters of isotherm adsorption models for adsorption of cadmium metal ions on iron oxide and TOPO functionalized iron oxide nanoparticles at 25 °C and different pH ranges, i.e., 5, 6, 7, and 8

pH range	Langmuir parameters			Freundlich parameters		
	R^2	Q_m	b	Q	R^2	Kf
For FeO 2 mg/20 ml cadmium metal ion						
pH5	0.9983	0.166378278	121.4222222	0.747216618	0.9987	0.51315184
pH6	0.956	0.00569152	22.87909369	0.108225108	0.9871	0.690634577
pH7	0.4123	0.033217074	42.68396427	0.356544372	0.7849	0.542421722
pH8	0.8393	0.03307097	275.8941606	0.611845326	0.8777	0.33735835
For FeO 4 mg/40 ml						
pH6	0.8174	0.025609506	25.20364035	0.233198078	0.9243	0.661055358
For FeO TOPO 2 mg/20 ml						
pH5	0.5385	0.000342924	16.18257492	0.035028724	0.8503	0.799820693
pH6	0.9818	0.060642814	22.68225585	0.303214069	0.9928	0.704987067
pH7	0.895	0.011433929	62.36380491	0.233486656	0.9578	0.501628016
pH8	0.8748	0.002161928	93.2184603	0.138881173	0.9412	0.464811826
For FeO TOPO 4 mg/40 ml						
pH6	0.7422	0.022330899	39.97232884	0.266716454	0.9133	0.569819751

linear plots of C_e versus C_e/q_e in (Fig. 6a–d). Values of q_m and b are represented in Tables 2 and 3, respectively. The isotherm was found to be linear in most of the concentration ranges studies displaying with best linear correlation values $R^2 = 0.9995$ and 0.9993 for nickel when adsorbed to IONPs and TF IONPs, respectively. Whereas correlation values were $R^2 = 0.9983$ and 0.9818 for cadmium adsorption to IONPs and TF IONPs. Thus, confirming the monolayer coverage of cadmium and nickel (pollutants) on the applied sorbents, i.e., IONPs and TF IONPs respectively.

Freundlich isotherm

While Langmuir isotherm says that enthalpy of adsorption does not depend on concentration of metal ions adsorbed, the empirical Freundlich isotherm equation which is based on adsorption on heterogeneous sites can be derived by supposing a logarithmic decrease in the enthalpy of adsorption with the increase in the number of adsorption sites (Meroufel et al. 2013). The Freundlich isotherm suggests adsorption phenomena to occur on heterogeneous surfaces (Ayawei et al. 2017). Mathematical form of Freundlich equation is given as:

$$q_e = KfC_e(1/n) \tag{10}$$

$$\text{Linearized form}: \quad \log q_e = \log Kf + (1/n) \log C_e \tag{11}$$

where kf is adsorption capacity (L/mg), and $1/n$ is adsorption intensity. It also indicates relative distribution of energy and the heterogeneity of adsorbates. Both kf and $1/n$ are Freundlich constants. These are calculated from the slope and intercept of graph logqe vs. log Ce which are shown in Fig. 7a–d, respectively. The parameters for Freundlich model are jotted down in Tables 2 and 3, respectively. Comparing the results of regression coefficient values for nickel and cadmium, we can find best R^2 values for nickel equal to 1 in case of TOPO functionalized iron oxide showing that Freundlich isotherm fitted best for the experimental data in case of nickel adsorption (Zhang et al. 2020). On the other hand, best R^2 values of cadmium are found to be 998 for adsorption on IONPs and 992 for adsorption on TF IONPs. Overall we can find that R^2 values of Freundlich model for both the metals are best as compared to Langmuir model which reveals that the data best fits for Freundlich model. This explains the process of adsorptions to occur at heterogeneous sites on both the adsorbents IONPs and TF IONPs. In addition, the adsorption sites also carry different energies (Shahriari et al. 2019).

Adsorption kinetics

Kinetic models help to access the time of stock piling of heavy metals on the surface of adsorbent consequently aiding in revealing the rate of adsorption (Samad et al. 2020). Chemical kinetics are very important to know about the rate constants of reaction and to determine whether the adsorption process takes place quickly or slowly (Adane et al. 2015). In order to conduct the kinetic study of nickel and cadmium removal by IONPs and TF IONPs, experimental data were used for pseudo-first-order and pseudo-second-order kinetic model. Overall the rate of cadmium and nickel adsorption was relatively higher in early stages but gradually decreased over time when equilibrium was achieved. This can be due to the high availability of active sites in initial stages and gradually over time these active sites get packed

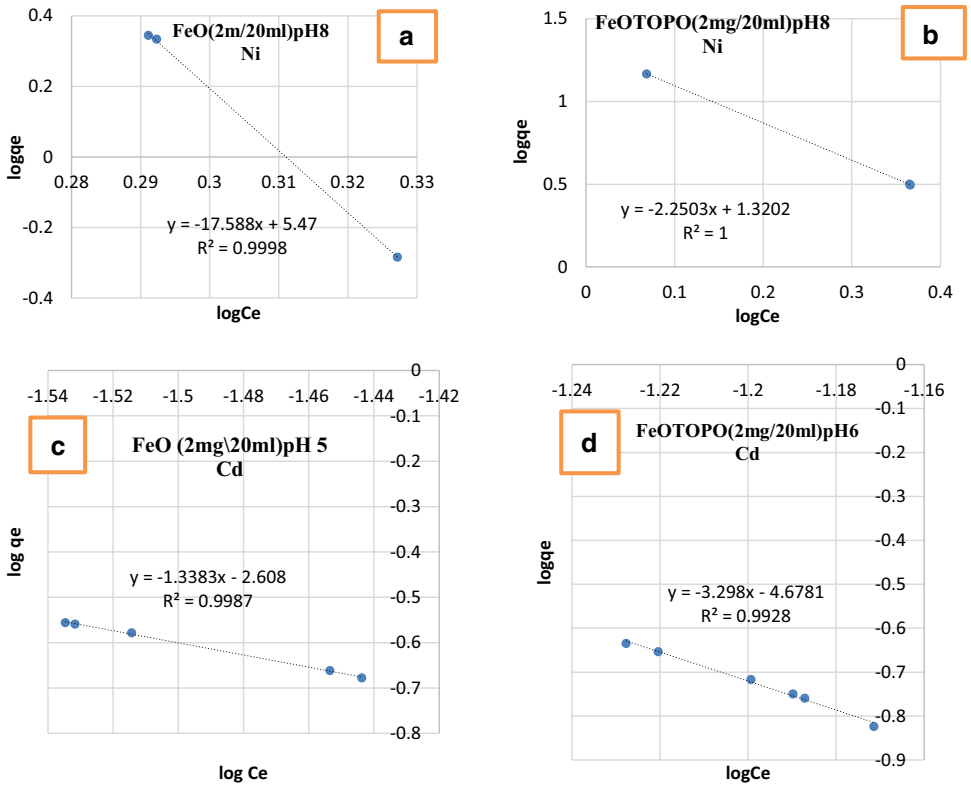

Fig. 7 Freundlich isotherm plots for adsorption of (**a**) Magnetite NPs (2 mg/20 ml) to Ni at pH8, (**b**) TOPO coated magnetite NPs (2 mg/20 ml) to Ni at pH8, (**c**) magnetite NPs (2 mg/20 ml) to Cd at pH5, (**d**) TOPO coated magnetite NPs to Cd at pH 6

with nickel and cadmium creating lower number of active sites for further adsorption due to which the rate of adsorption decreases (Duarte Neto et al. 2018).

Pseudo-first-order kinetics (Langergren's)

Pseudo-first-order kinetic model was applied to study the rate of adsorption of nickel and cadmium ion on IONPs and TF IONPs at equilibrium or at any time. Pseudo-first-order kinetics undergoes physisorption process (Gusain et al. 2019) and is represented mathematically in Eq. (12).

$$\log\left(q_e - q_t\right) = \log -K_1 t/2.303 \tag{12}$$

where q_e and q_t are amounts of adsorbates (mg/g) at equilibrium, and time t (s) $K1$ is the rate constant of pseudo-first-order kinetics. The plot log (q_e–q_t) versus time (t) gives a straight line that finds $K1$ and q_e from slope and intercept. The respective plots for pseudo-first-order are shown in Fig. 8a–d. Values of $k1$ and regression coefficient are jotted down in Tables 4 and 5 for nickel and cadmium adsorption by the two types of adsorbents. Comparing the values of regression coefficient, we get best values of $R2$ at higher adsorbent doses (4 mg/40 ml) of IONPs equal to 0.935 at pH 6 for nickel adsorption, and for TF IONP (4 mg/40 ml) sample, we get R^2 value equal to 0.932 at pH 6. Whereas for cadmium metal adsorption, the R^2 value was found to be 0.943 at 2 mg/20 ml at pH 8 when adsorbed to IONPs sample and R^2 value was 0.9708 for TF IONPs (2 mg/20 ml concentration) at pH5. These values indicate that at such pH values and concentration of adsorbent, the process of kinetic adsorption favors physisorption phenomena.

Pseudo-second-order model

Pseudo-second-order kinetics follows chemisorption process. Linearized form of pseudo-second-order kinetics is given in Eq. (13)

$$t/q_t = 1/K_2 q_e^2 + 1t/q_t \tag{13}$$

where $K2$ is the rate constant for pseudo-second-order model mg/g per minute. Value of $K2$ depends on experimental conditions such as initial pH and solution agitation rate, temperature and concentration. The value of $k2$ lowers with increasing concentration of solution as it takes longer time to attain the equilibrium (Aly et al. 2014).

Pseudo-second-order plots t/q_t versus time (min) gave a straight line as indicated in Fig. 8e, f. The values of $k2$, q_e and R^2 are calculated from the plots and jotted down in Tables 4 and 5, respectively. The linear correlation coefficient values are higher, i.e., 0.98 for sample TF IONPs (2 mg/20 ml) at pH 6 for adsorption nickel and 0.96 for IONPs (2 mg/20 ml) sample at pH5 for cadmium metal

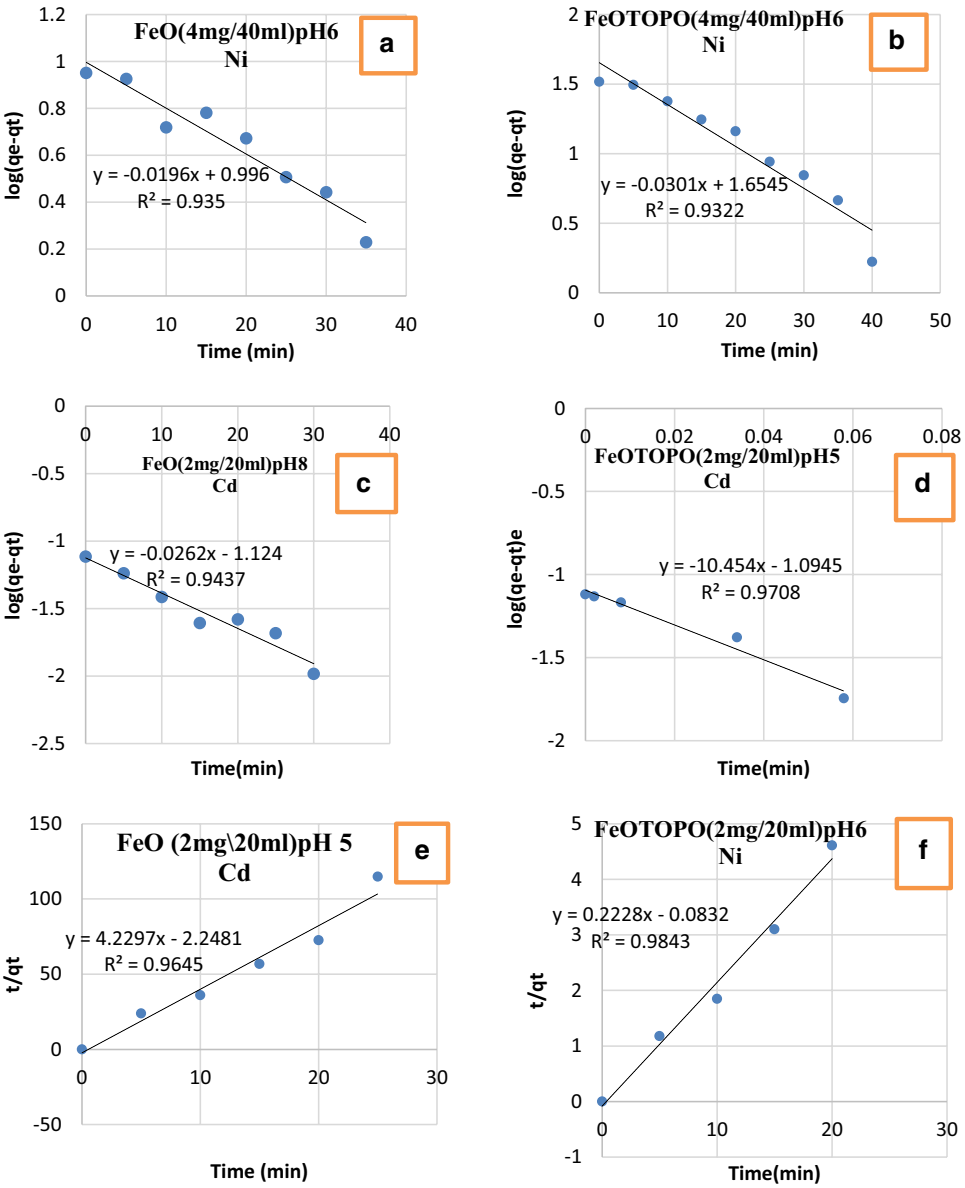

Fig. 8 Pseudo 1st (**a**, **b**, **c**, **d**) and 2nd order (**e**, **f**) plots for adsorption of (**a**) Magnetite NPs (4 mg/40 ml) to Ni at pH 6, (**b**) TOPO coated magnetite NPs (4 mg/40 ml) to Ni at pH 6, (**c**) magnetite NPs (2 mg/20 ml) to Cd at pH8, (**d**) TOPO coated magnetite NPs to Cd at pH 5, (**e**) magnetite NPs (2 mg/20 ml) to Cd at pH5 (**f**) TOPO coated magnetite NPs (2 mg/20 ml) to Ni at pH6

adsorption. Additionally, the values of q_e (cal), i.e., calculated adsorption capacity were not in close agreement with the experimental adsorption capacity revealing that removal of metal ions by adsorbent followed pseudo-second-order. The data suggest the chemisorption process, and it might be due to the exchange of metal ions with the functional groups of iron oxide NPs and TOPO functionalized iron oxide NPs (Cheng et al. 2020).

Effect of different parameters on adsorption of metal ions onto sorbent surface

The results generated overall from isotherm and kinetic models give us a clear indication that while working with IONPs and TF IONPs one can clearly observe fluctuations in adsorption capacities as being directly influenced by different values of pH, i.e., different conditions of acidic and basic environments. Apart from this effect of adsorbent dose and contact time was also studied that was found to have a notable influence upon the adsorption capacity.

Effect of pH

pH value is one of the most crucial factors that governs the binding of heavy metal ions on the surface of adsorbents since the hydrogen ions concentration has the direct consequence on the adsorption sites of the adsorbent (Ouyang et al. 2019). The effect of pH on the removal of Ni^{2+} and Cd^{2+} through IONPs and TF IONPs was studied by adjusting the pH in the range of 5–8 by adding 0.1 M HCl and

Table 4 Parameters of kinetic adsorption models for adsorption of nickel metal ions on iron oxide and TOPO functionalized iron oxide nanoparticles at 25 °C and different pH ranges, i.e., 5, 6, 7, and 8

pH range	Pseudo-first-order parameters			Pseudo-second-order parameters		
	R^2	$K1$	q_e	$K2$	h	$R2$
For FeO 2 mg/20 ml nickel metal ion						
pH5	0.6361	0.0787626	1.871607711	0.005131424	0.017974943	0.0051
pH6	0.8859	0.2436574	6.26566416	0.000797035	0.043092304	0.0028
pH7	0.7735	0.0693203	8.787346221	0.036023477	2.781641168	0.8055
pH8	0.8039	0.3712436	3.249918752	0.032067499	0.33869602	0.2398
For FeO 4 mg/40 ml						
pH6	0.935	0.0451388	37.59398496	0.000175199	0.247610558	0.0284
For FeO TOPO 2 mg/20 ml						
pH5	0.7979	0.080605	1.569119724	0.028461898	0.070077085	0.1407
pH6	0.5476	0.078302	4.488330341	0.596632692	12.01923077	0.9843
pH7	0.8724	0.0099029	1.496781919	0.153024653	0.342829716	0.1763
pH8	0.6288	0.0147392	8.554319932	0.013377983	0.978952521	0.2557
For FeO TOPO 4 mg/40 ml						
pH6	0.9322	0.0693203	59.52380952	0.000159458	0.564971751	0.1486

Table 5 Parameters of kinetic adsorption models for adsorption of cadmium metal ions on iron oxide and TOPO functionalized iron oxide nanoparticles at 25 °C and different pH ranges i.e. 5, 6, 7, and 8

pH range	Pseudo-first-order parameters			Pseudo-second-order parameters		
	R^2	$K1$	q_e	$K2$	h	$R2$
For FeO 2 mg/20 ml cadmium metal ion						
pH5	0.0952	0.1524586	0.236423387	7.957992122	0.44482007	0.9645
pH6	0.8355	0.0449085	0.069749599	2.671278903	0.012995789	0.7437
pH7	0.6229	0.0262542	1.337971635	0.002262207	0.004049731	0.0024
pH8	0.9437	0.0603386	0.087627059	1.090278309	0.008371704	0.8192
For FeO 4 mg/40 ml						
pH6	0.8596	0.0983381	0.144383483	0.983747098	0.020507772	0.3605
For FeO TOPO 2 mg/20 ml						
pH5	0.9708	24.075562	0.046609182	0.330806342	0.000718649	0.011
pH6	0.7851	0.0969563	0.23549914	1.554536054	0.086214329	0.9536
pH7	0.8786	0.0882049	0.084317032	1.670382861	0.011875356	0.8502
pH8	0.7355	0.0497448	0.008899964	3.538133961	0.000280253	0.0582
For FeO TOPO 4 mg/40 ml						
pH6	0.7554	0.066787	0.67114094	0.01497134	0.006743543	0.0888

0.1 M NaOH to the metal ion solutions. The present study showed that the removal of cadmium and nickel ion was highly dependent on pH conditions. Results from Langmuir data showed that the amounts of Ni cation concentrations adsorbed to iron oxide were found to be lesser at lower pH values. Good adsorbability was obtained in the case of TF IONPs adsorbent. The steady values achieved for TOPO functionalized nanoadsorbents were 1.1 mg/g at pH5, 2.7 mg/g at pH6, 2.2 at pH7, and 14 mg/g at pH 8. This can be explained by the fact that the Ni^{2+} ions start to compete with active sites of adsorbent at lower pH. With increased pH as for in the case of TOPO functionalization, the P=O groups become free due to undoping thus resulting in efficient removal of Ni^{2+} ions. Less adsorption of nickel in strong acidic or basic conditions might be due to the presence of electrostatic interactions created due to $Ni(OH)_3^-$ and $Ni(OH)^+$ ions in the solution (Muhammad et al. 2020). On the other hand, Langmuir data for cadmium show that the adsorption capacities were found to be higher even at low pH ranges, i.e., q_e values were 8.0 mg/g at pH 5 and 3.5 mg/g at pH 8. This is due to the fact that oxygen-containing functional groups on the surface of adsorbent gets ionized hence aiding in adsorption (Sitko et al. 2013).

Effect of contact time

Contact time was maintained at 0–50 min for samples recorded at pH 5, 6, 7 and 8 with 2 mg/ml concentration of both the adsorbents and 0–100 min for samples recorded at pH6 with 4 mg/ml of adsorbent concentration.

The adsorption capacities on the proposed time intervals showed that values of qe were greater initially, and then, with the lapse of time, the adsorption decreased. This can be explained due to the fact that as the time increases the number of available active sites of adsorbents that gets occupied by the heavy metal ions results in saturation of sorbent surface and decreasing the pore diffusion of the ions (Kahrizi et al. 2018; Hosseini et al. 2019).

Effect of adsorbent dose

The adsorbent dose was set at two concentrations which were 2 mg/ml and 4 mg/ml doses of adsorbent at pH 6. The results showed that adsorbent dose has an impact on the Qm values in case of nickel metal adsorption. The Q_m values were recorded to be lesser, i.e., 0.0031 at 2 mg dose of adsorbent (IONP) and greater, i.e., 0.315 at 4 mg adsorbent (IONP) dose. For TOPO functionalized adsorbent sample, the Q_{m} value was found to be 0.8 at 2 mg dose and quite greater, i.e., 4.7 at 4 mg/ml of adsorbent dose. As the adsorbent dosage increases, the number of available active sites tends to be greater thus providing greater number of sites for the metal ions to attach. (Phuengprasop et al. 2011). In case of cadmium adsorption, the adsorbent dose was found to have no impact on adsorption efficiency. This might be due to the electrostatic repulsions between the metal cations possibly causing hindrance in the adsorption of metal ions (Razzaq et al. 2020). While determining the effect of dose other variables (pH 5, 7, 8), and contact time was kept constant.

Conclusion

Iron oxide nanoparticles are research suitable nanoparticles that are found to be most useful in removing heavy metal contaminants due to their magnetic properties. Trioctyl phosphine oxide on the other hand is used a surface functionalization agent and a good extractant for the recovery of radioactive waste such as uranium metal. The present study was aimed keeping in front the magnetic properties of Fe_3O_4 NPs and extractant ability of TOPO to remove heavy metals such as Ni^{2+} and Cd^{2+} cations in synthetic wastewater. The two adsorbents Fe_3O_4 NPs and TOPO bound Fe3O4 NPs were tested for their adsorption capacities by providing different pH conditions such as at pH 5, 6, 7 and 8. It was found that Fe3O4 NP's and TOPO bound Fe3O4 NPs shows better adsorption capacities at basic conditions, i.e., equilibrium adsorption values were 14 mg/g for both the adsorbents in case of nickel cations. This is because at higher pH values, the functional groups of adsorbents get free resulting in efficient attachment to heavy metal ions thus giving higher adsorption values. The adsorption capacities of the relevant time intervals showed that values of qe were greater initially and then decreases gradually because of the fact that when time increases the number of available active sites of adsorbents gets occupied by the heavy metal ions resulting in saturation of sorbent surface and decreasing the pore diffusion of the ions. Higher adsorption values were observed for Ni^{2+} adsorption at higher concentrations of both bare and TOPO coated Fe_3O_4 NPs. The R^2 values of Freundlich isotherm model were higher as compared to Langmuir model which shows the data best fitted to Freundlich isotherm which indicates that the process of adsorption occurs at heterogeneous sites on the surface of Fe_3O_4 NPs and TOPO bound Fe_3O_4 NPs. On the other hand, the R^2 values for Cd^{2+} and Ni^{2+} showed the data best fitted to pseudo-second-order model. Finally, it can be concluded that TOPO functionalization of Fe_3O_4 NPs proves to be a satisfactory approach in remediating contaminants from wastewater.

Funding The author(s) received no specific funding for this work.

Declarations

Conflict of interest Authors declare no competing interest and affirm that they have no known competing financial interests or personal relationships that could have appeared to influence the work reported in this paper.

References

Adane B, Siraj K, Meka N (2015) Kinetic, equilibrium and thermodynamic study Of 2-chlorophenol adsorption onto ricinus communis pericarp activated carbon from aqueous solutions. Green Chem Lett Rev 8(3–4):1–12

Al-Saad KA, Amr MA, Hadi DT, Arar RS, Al-Sulaiti MM, Abdulmalik TA, Alsahamary NM, Kwak JC (2012) Iron oxide nanoparticles: applicability for heavy metal removal from contaminated water. Arab J Nuclear Sci Appl 45(2):335–346

Aly Z, Graulet A, Scales N, Hanley T (2014) Removal of aluminium from aqueous solutions using pan-based adsorbents: characterisation, kinetics, equilibrium and thermodynamic studies. Environ Sci Pollut Res 21(5):3972–3986

Arenas-Alatorre J, Lukas O, Rodríguez-Gómez A, Reyes RH, Tapia-Del León C (2019) Synthesis and characterization of iron oxide nanoparticles grown via a non-conventional chemical method using an external magnetic field. Mater Lett 242:13–16

Ayawei N, Ebelegi AN, Wankasi D (2017) Modelling and interpretation of adsorption isotherms. J Chem. https://doi.org/10.1155/2017/3039817

Baragaño D, Forján R, Welte L, José-Gallego LR (2020) Nanoremediation of as and metals polluted soils by means of graphene oxide nanoparticles. Sci Rep. https://doi.org/10.1038/S41598-020-58852-4

Bardos P, Bone B, Černík M, Elliott DW, Jones S, Merly C (2015) Nanoremediation and international environmental restoration markets. Remediat J 25(2):83–94

Batool F, Akbar J, Iqbal S, Noreen S, Bukhari SNA (2018) Study of isothermal, kinetic and thermodynamic parameters for adsorption of cadmium: an overview of linear and nonlinear approach and error analysis. Bioinorg Chem Appl. https://doi.org/10.1155/2018/3463724

Batra S, Datta D (2019) Removal of bisphenol-a from aqueous solution using polymeric resin impregnated with phosphorous based extractant. Int J Chem Eng Appl 10(3):87

Chemical Book, TOPO (2017). https://Www.Chemicalbook.Com/Chemicalproductproperty_En_Cb3268225.Htm

Chen X (2015) Modeling of experimental adsorption isotherm data. Information 6(1):14–22

Cheng Y, Wang K, Tu B, Xue S, Deng J, Tao H (2020) Adsorption of divalent cadmium by calcified iron-embedded carbon beads. RSC Adv 10(11):6277–6286

Chowdhury S, Misra R, Kushwaha P, Das P (2011) Optimum sorption isotherm by linear and nonlinear methods for safranin onto alkali-treated rice husk. Bioremediat J 15(2):77–89

Dada AO, Olalekan AP, Olatunya AM, Dada OJIJC (2012) Langmuir, freundlich, temkin and dubinin-radushkevich isotherms studies of equilibrium sorption of Zn2+ unto phosphoric acid modified rice husk. Iosr J Appl Chem 3(1):38–45

Desta MB (2013) Batch sorption experiments: langmuir and freundlich isotherm studies for the adsorption of textile metal ions onto teff straw (Eragrostis Tef) agricultural waste. J Thermodyn. https://doi.org/10.1155/2013/375830

Duarte Neto JF, Pereira IDS, Da Silva VC, Ferreira HC, Neves GDA, Menezes RR (2018) Study Of equilibrium and kinetic adsorption of rhodamine B onto purified bentonite clays. Cerâmica 64(372):598–607

Duruibe JO, Ogwuegbu MOC, Egwurugwu JN (2007) Heavy metal pollution and human biotoxic effects. Int J Phys Sci 2(5):112–118

Gheorghe S, Stoica C, Vasile GG, Nita-Lazar M, Stanescu E, Lucaciu IE (2017) Metals toxic effects in aquatic ecosystems: modulators of water quality. Water Qual. https://doi.org/10.5772/65744

Gusain R, Kumar N, Fosso-Kankeu E, Ray SS (2019) Efficient removal Of Pb (Ii) and Cd (Ii) from industrial mine water by a hierarchical Mos2/Sh-Mwcnt nanocomposite. ACS Omega 4(9):13922–13935

Ho YS, Mckay G (1999) Pseudo-second order model for sorption processes. Process Biochem 34(5):451–465

Hosseini R, Sayadi MH, Shekari H (2019) Adsorption of nickel and chromium from aqueous solutions using copper oxide nanoparticles: adsorption isotherms, kinetic modeling, and thermodynamic studies. Avicenna J Environ Health Eng 6(2):66–74

Jaishankar M, Tseten T, Anbalagan N, Mathew BB, Beeregowda KN (2014) Toxicity, mechanism and health effects of some heavy metals. Interdiscip Toxicol 7(2):60–72

Kahrizi P, Mohseni-Shahri FS, Moeinpour F (2018) Adsorptive removal of cadmium from aqueous solutions using Nife 2 O 4/hydroxyapatite/graphene quantum dots as a novel nano-adsorbent. J Nanostruct Chem 8(4):441–452

Khajavian M, Wood DA, Hallajsani A, Majidian N (2019) Simultaneous biosorption of nickel and cadmium by the brown algae cystoseria indica characterized by isotherm and kinetic models. Appl Biol Chem 62(1):1–12

Kinniburgh DG (1986) General purpose adsorption isotherms. Environ Sci Technol 20(9):895–904

Li Q, Kartikowati CW, Horie S, Ogi T, Iwaki T, Okuyama K (2017) Correlation between particle size/domain structure and magnetic properties of highly crystalline Fe_3o_4 nanoparticles. Sci Rep 7(1):1–7

Lim YS, Lai CW, Hamid SBA, Julkapli NM, Yehya WA, Karim MZ, Lau KS (2014) A study on growth formation of nano-sized magnetite Fe_3o_4 via co-precipitation method. Mater Res Innov 18(Sup6):S6-457

Masindi V, Muedi KL (2018) Environmental contamination by heavy metals. Heavy Metals 10:115–132

Mazrouaa AM, Mohamed MG, Fekry M (2019) Physical and magnetic properties of iron oxide nanoparticles with a different molar ratio of ferrous and ferric. Egypt J Pet 28(2):165–171

Mohammed AS, Kapri A, Goel R (2011) Heavy metal pollution: source, impact, and remedies. Biomanagement of metal-contaminated soils. Springer, Dordrecht, pp 1–28

Muhammad A, Bilal S (2020) Effective adsorption of hexavalent chromium and divalent nickel ions from water through polyaniline, iron oxide and their composites. Appl Sci 10(8):2882

Meroufel B, Benali O, Benyahia M, Benmoussa Y, Zenasni MA (2013) Adsorptive removal of anionic dye from aqueous solutions by Algerian Kaolin: characteristics, isotherm, kinetic and thermodynamic studies. J Mater Environ Sci 4(3):482–491

Nassar NN (2012) Iron oxide nanoadsorbents for removal of various pollutants from wastewater: an overview. Appl Adsorb Water Pollut Control. https://doi.org/10.2174/97816080526911120101 0081

National Library Of Medicine, Pubchem](Nd). https://Pubchem.Ncbi.Nlm.Nih.Gov/Compound/Trioctylphosphine-Oxide

Ouyang D, Zhuo Y, Hu L, Zeng Q, Hu Y, He Z (2019) Research on the adsorption behavior of heavy metal ions by porous material prepared with silicate tailings. Minerals 9(5):291

Petcharoen K, Sirivat A (2012) Synthesis and characterization of magnetite nanoparticles via the chemical Co-precipitation method. Mater Sci Eng B 177(5):421–427

Phuengprasop T, Sittiwong J, Unob F (2011) Removal of heavy metal ions by iron oxide coated sewage sludge. J Hazard Mater 186(1):502–507

Rahbaralam M, Abdollahi A, Fernàndez-Garcia D, Sanchez-Vila X (2020) Stochastic modeling of non-linear adsorption with Gaussian kernel density estimators. Arxiv Preprint Arxiv: http://arxiv.org/abs/2004.06445

Rajendran K, Sen S (2018) Adsorptive removal of carbamazepine using biosynthesized hematite nanoparticles. Environ Nanotechnol Monit Manag 9:122–127

Razzaq R, Shah KH, Fahad M, Naeem A, Sherazi TA (2020) Adsorption potential of macroporous amberlyst-15 For Cd (Ii) removal from aqueous solutions. Mater Res Exp 7(2):025509

Rusianto T, Wildan MW, Abraha K (2015) Various sizes of the synthesized Fe_3O_4 nanoparticles assisted by mechanical vibrations. Indian J Eng Mater Sci 22:175

Samad A, Din MI, Ahmed M (2020) Studies on batch adsorptive removal of cadmium and nickel from synthetic waste water using silty clay originated from Balochistan-Pakistan. Chin J Chem Eng 28(4):1171–1176

Sardar K, Ali S, Hameed S, Afzal S, Fatima S, Shakoor MB, Tauqeer HM (2013) Heavy metals contamination and what are the impacts on living organisms. Greener J Environ Manag Public Saf 2(4):172–179

Shahriari T, Mehrdadi N, Tahmasebi M (2019) Study of cadmium and nickel removal from battery industry wastewater by Fe_2o_3 nanoparticles. Pollution 5(3):515–524

Simonin JP (2016) On the comparison of pseudo-first order and pseudo-second order rate laws in the modeling of adsorption kinetics. Chem Eng J 300:254–263

Singh MR, Gupta A (2016) Water pollution-sources, effects and control. Centre for Biodiversity, Department Of Botany, Nagaland University

Singh J, Kalamdhad AS (2011) Effects of heavy metals on soil, plants, human health and aquatic life. Int J Res Chem Environ 1(2):15–21

Sitko R, Turek E, Zawisza B, Malicka E, Talik E, Heimann J, Wrzalik R (2013) Adsorption of divalent metal ions from aqueous solutions using graphene oxide. Dalton Trans 42(16):5682–5689

Sogut EG, Caliskan N (2017) Isotherm and kinetic studies of Pb (Ii) adsorption on raw and modified diatomite by using non-linear regression method. Fresenius Environ Bull 26(4):2721–2729

Srivastava V, Sarkar A, Singh S, Singh P, De Araujo AS, Singh RP (2017) Agroecological responses of heavy metal pollution with special emphasis on soil health and plant performances. Front Environ Sci 5:64

Terdputtakun A, Arqueropanyo OA, Sooksamiti P, Janhom S, Naksata W (2017) Adsorption isotherm models and error analysis for single and binary adsorption Of Cd (Ii) and Zn (Ii) using leonardite as adsorbent. Environ Earth Sci 76(22):777

Vardhan KH, Kumar PS, Panda RC (2019) A review on heavy metal pollution, toxicity and remedial measures: current trends and future perspectives. J Mol Liquids 290:111197

Walter A, Garofalo A, Parat A, Martinez H, Felder-Flesch D, Begin-Colin S (2015) Functionalization strategies and dendronization of iron oxide nanoparticles. Nanotechnol Rev 4(6):581–593

Watson EK, Rickelton WA (1992) A review of the industrial and recent potential applications of trioctylphosphine oxide. Solvent Extr Ion Exch 10(5):879–889

Xu Y, Qin Y, Palchoudhury S, Bao Y (2011) Water-soluble iron oxide nanoparticles with high stability and selective surface functionality. Langmuir 27(14):8990–8997

Zhang J, Zhao SQ, Zhang K, Zhou JQ, Cai YF (2012) A study of photoluminescence properties and performance improvement of Cd-doped Zno quantum dots prepared by the sol–gel method. Nanoscale Res Lett 7(1):1–7

Zhang M, Yin Q, Ji X, Wang F, Gao X, Zhao M (2020) High and fast adsorption of Cd (Ii) And Pb (Ii) ions from aqueous solutions by a waste biomass based hydrogel. Sci Rep 10(1):1–13